Research Article
Hittite Journal of Science and Engineering, 2023, 10 (2) 91–97
ISSN NUMBER: 2149–2123
DOI: : 10.17350/HJSE19030000306

The Performance Comparison of SC-PPM Receiver Models

Mehmet Sönmez
Osmaniye Korkut Ata University, Department of Electrical and Electronics Engineering, Osmaniye, Türkiye

ABSTRACT

This paper describes a physical layer solution to provide data transmission in the VLC networks. In the paper, it is aimed to examine the performance comparison of SC-PPM (Subcarrier Pulse Position Modulation) demodulator schemes. Three receiver techniques have been considered to assemble demodulator techniques to the SC-PPM receiver system. Firstly, the traditional PPM (T-PPM) demodulator has been applied to the SC-4PPM receiver system to estimate the slot that includes high-frequency signal that is referred to as subcarrier signal. To successfully detect the data signal using a traditional PPM receiver, it must be known the dimming level of the received SC-4PPM signal. In another receiver model that is referred to as PD (Peak Detector), it is aimed to detect peak values of slot filled by high frequency signal. The disadvantage of this system is that BER (Bit Error Rate) performance depends on the difference between the peak and bottom values of the subcarrier-filled slot. Hence, the second method is improved to achieve a similar BER performance at all dimming levels between 12.5% and 87.5%. This receiver model is called IPD in the paper. In brief, it is reported for the first time, it has been employed the PD and the IPD algorithms for the SC-PPM receiver schemes. In addition to this, it is given a theoretical framework for both the traditional PPM and the improved receiver schemes in VLC-SC-PPM schemes. Moreover, it has been investigated how the SC-PPM receiver schemes are affected by brightness level.

Keywords:
SC-PPM, VLC, Detection, Dimming level

Article History:
Received: 2022/04/27
Accepted: 2023/05/12
Online: 2023/06/30

***Correspondence to**: Mehmet Sönmez,*
E-Mail: mehmetsonmez@osmaniye.edu.tr
Phone: +9 032 882 710 00

This article has been checked for similarity.

INTRODUCTION

Visible light communication (VLC) technology has arisen as a promising candidate to solve the critical challenges of wireless communication networks. In particular, the evolving explosion in the use of internet services requiring high bandwidth will soon become a great potential problem among service providers. In the context of sharing huge data, visible light communication (VLC) has been conjectured to be a leading potential solution to meet the demands of the sixth-generation (6G) and beyond networks by researchers from both academia and industry (1-3). To ensure data transmission in the physical layer of wireless networks, however, there are some critical challenges (4, 5). In particular, there are research issues carried out by various researchers to investigate and improve the data transmission techniques (6-9).

To meet the high-speed data rate demands of upcoming 6G mobile wireless networks, VLC has been investigated from several aspects for integration into these mobile technologies (10, 11). In the literature, some authors have focused on the hybrid and heterogeneous mobile networks to assure the demands of users and service providers (12-17). In addition to providing high data rate, energy-efficient schemes have been attracted the very attention from researchers (18-19). Specifically, IoT (Internet of Things) technology which is one of the backbones of industrial systems has been recently combined to VLC systems to provide energy efficiency [19]. Moreover, channel modelling and indoor positioning are very attractive issues for VLC systems such as RF systems (20-23).

In the VLC systems, energy efficiency can also be ensured by using dimming control techniques such as modulation-based methods (24). The VPPM (Variable Pulse Position Modulation) and VOOK (Variable On-Off Keying) transmission schemes are leading techniques to control LED (Light Emitting Diode) brightness (25). In addition to these schemes, the SC-PPM scheme ensures dimming control of LED by mostly using a DC (Direct Current) signal for empty slots. Moreover, this

transmission technique adjusts the dimming level by employing the difference between the peak and bottom values of the subcarrier signal slot (26, 27). Just as the dimming level can be controlled by adjusting the duty cycle of the modulated signal, it can be regulated by attaching a sequential '1' or '0' bit array to the main modulated signal. This attached array is referred to as Compensation Time (CT) (28). Addition to CT method, dimming compensator schemes have been also proposed to achieve dimmable VLC systems that are including forward error correction (FEC) techniques (29). As mentioned above, many researchers have focused on improving dimming methods to provide both energy efficiency and data transmission in VLC technology. Therefore, it can be remarked that it is very important to investigate modulation-based dimming techniques such as SC-PPM to observe their BER performances.

Compared with the PPM transmission scheme, the SC-PPM method has better performance in terms of energy consuming (30). To maintain the energy efficiency of the SC-PPM system, the adjusting dimming level of the SC-PPM scheme was asserted as an optimization problem by authors of (31). In the paper, the BER performance was investigated by taking into account the required power consumption that was achieved by optimizing the modulation index of the signal. Another optimization problem was described by the authors of (32). In order to increase the signal-to-noise ratio (SNR), the paper suggested a linear dimming control model to apply the SC-4PPM transmission scheme. In other words, it was aimed to achieve optimal SNR performance at the provided dimming level. These authors asserted that energy saving can be ensured by employing an optimized SC-PPM scheme for dimmable VLC systems in another paper. According to simulation results, it was demonstrated that the optimized SC-PPM scheme could save more than 40% of energy by investigating the tradeoff between energy efficiency and SNR (33). In addition to these papers, an experimental study which is based on FPGA (Field Programmable Gate Arrays) board was presented in the literature (34). The paper reported practicable both a modulator structure and a demodulator architecture.

This paper has investigated the performance analysis of SC-PPM receiver models to determine the optimum demodulator scheme that detects data bits from received SC-PPM signals. Firstly, a traditional PPM receiver model is applied to the SC-PPM receiver scheme to observe the BER performance. However, it can be stated that this receiver doesn't suitable to demodulate SC-PPM signals for real-time systems since it needs the dimming level knowledge of the received SC-PPM signal. Hence, it is necessary either a dimming estimation method or a knowledge of the dimming level of the received SC-PPM signal at the receiver side. In order the cope with these challenges, the PD method is applied to the SC-PPM receiver scheme. This scheme uses peak values of the subcarrier signal to detect the data bits. The BER performance is decreasing when increased the dimming level of the SC-PPM signal since the difference between the peak value of the subcarrier signal and the peak value of the DC signal is decreased. Therefore, the PD method is improved to eliminate this problem. The improved scheme is referred to as the IPD model which gives similar BER performance at the dimming levels between 12.5% and 87.5%.

MATERIAL AND METHODS

It is briefly recapped the SC-PPM transmission scheme with the illustration in Fig. 1. The SC-PPM scheme consists of both DC level and subcarrier signal to encode data bits. According to the waveform given in Fig. 1, the dimming level between 12.5% and 87.5% can be adjusted by the b parameter which acts as a DC component. The c value changes the dimming level between 0% to 12.5% just as the a value controls the dimming level between 87.5% and 100%. To observe the parameters' effect on the dimming level, a theoretical expression can be given by (32),

$$d = (a + c)x0.125 + bx0.75 \quad (1)$$

where, d is defined as the dimming level of the SC-PPM signal. The a, b, and c can change from 0 to 1 (32).

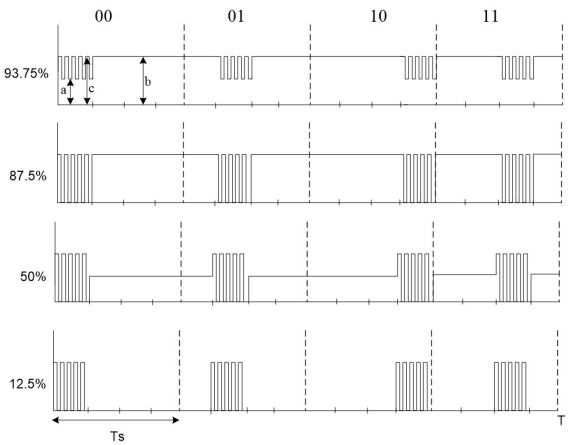

Figure 1. SC-4PPM signal waveform in terms of the time

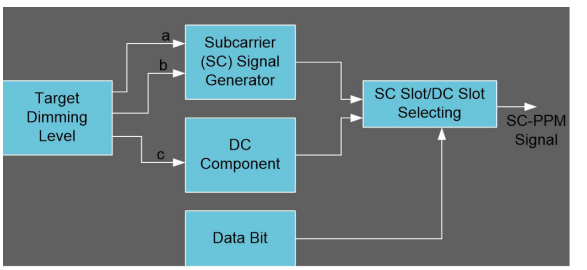

Figure 2. A block diagram to generate SC-4PPM signal

Fig. 2 illustrates a block diagram for the SC-PPM scheme that consists of two different signal conditions that are Subcarrier signal and the DC component. As given in the figure, dimming level control can be achieved to ensure the

target brightness level by adjusting a, b, and c parameters. The subcarrier signal adjusts the dimming control by employing levels of a and b while the DC component determines the target dimming level using the c parameter. The parameters of c and b can get up to A level, if the peak value of SC-PPM signal is A level under full brightness. The minimum value of these parameters is zero level. The parameter a can be adjusted from zero level up to A level. However, the transmission cannot be performed at these limit values due to full brightness and darkness. To determine the position of the SC Signal, it must be used position selecting process that is pointed out by the SC slot / DC slot selecting block in the figure. The position of the subcarrier signal is determined by taking into account the data bit condition.

DEMODULATOR SCHEMES FOR SC-PPM TECHNIQUE

Traditional PPM Demodulator

In this section, we have investigated the theoretical framework of demodulator schemes for the SC-PPM method. The section includes three demodulator techniques. The first technique is referred to as the traditional PPM demodulator scheme. The difficulty of this demodulator requires knowing the dimming level of the received SC-PPM signal. Additionally, it can be stated that traditional PPM cannot be implemented to SC-PPM demodulator at the 50% dimming level since the mean value of all slots is equal to each other at this dimming level. Hence, it is considered two dimming conditions: above 50% of the dimming level and below 50% of the dimming level. The slot time can be expressed by (35),

$$\boldsymbol{Ts = T_{sym} / M} \tag{2}$$

where, Ts and Tsym present slot time and symbol period, respectively. The M value can be expressed as modulation order. If the k is presented as bit number including one symbol, the M is equal to 2^k.

$$\boldsymbol{I^n_{T-PPM} = \int_{nTs}^{(n+1)Ts} S(t)dt \qquad ; n = \{0,1,2,.....,M-1\}} \tag{3}$$

where, S(t), can be defined as the received SC-PPM signal and the integral value of the SC-PPM signal from nTs to (n+1)Ts. According to Fig. 1, the a, b, and c can be defined as the peak value of the subcarrier signal and DC level, respectively. The integral values of the subcarrier signal can be assumed as follows:

$$\boldsymbol{I^n_{SC} = \frac{Ts/M}{Tsc} x(a+c)} \tag{4}$$

$$\boldsymbol{I^n_{DC} = \frac{Ts/M}{Tsc} xb} \tag{5}$$

where, and are defined as integral values of the subcarrier signal and DC component, respectively. If the dimming level of the received SC-PPM signal is above 50%, the b value must be bigger than a plus c. Otherwise, the big element must be a plus c. Therefore, the condition of < is provided under above 50% of the dimming level. Under below 50% of the dimming level, it must be valid for the condition of > . For two conditions as mentioned above, the symbol can be determined following the decision criterion:

Case-1: Let us consider that the dimming level of the received SC-PPM signal is below 50%.

In this case, the integral value given in Eq. (3) is the biggest for the subcarrier signal. Hence, the maximal integral value can determine the position of the filled slot that is including the subcarrier signal. If argmax(.) can be considered as a function that returns the index of the maximum element in the set, a decision criterion can be written by,

$$\boldsymbol{i = arg\,max\left\{I^n_{T-PPM}, I^{n+1}_{T-PPM}, ..., I^{M-1}_{T-PPM}\right\} \qquad ; n = 0} \tag{6}$$

where, the i value gives the number of the filled slot with the subcarrier signal if the first slot is defined as zeroth.

Case-2: Let us consider that the dimming level of the received SC-PPM signal is above 50%.

This case aims to find the minimum element among the integral values of slots since the integral value of the DC component is bigger than that of the subcarrier signal.

$$\boldsymbol{i = arg\,min\left\{I^n_{T-PPM}, I^{n+1}_{T-PPM}, ..., I^{M-1}_{T-PPM}\right\} \qquad ; n = 0} \tag{7}$$

where, argmin(.) is used to indicate a function that returns the index of minimum element in the set. The BER performance of the SC-PPM is affected from both dimming cases since the integral results are determined by taking account a, b, and c parameters that aid to adjust dimming level of the SC-PPM. If the difference between b and (a+c) is increasing, it has been achieved better BER performance.

Peak Detector Based Demodulator

The Peak Detector-based demodulator provides to take the integration process through c values. In other words, this demodulator aims to detect the maximum value obtained among integrators that have taken into account c value. Consequently, an explanation for peak detector can be given by,

$$\boldsymbol{I^n_{Pd} = \int_{nTs}^{(n+1)Ts} S(t)S_{SC}(t)dt \qquad ; n = \{0,1,2,.....,M-1\}} \tag{8}$$

where, SSC(t) can be defined as a subcarrier signal in which the a value is equal to zero. This signal is given to present the masking process in Eq. (8). In the simulation or the experimental processes, it is adequate to take the partial integral through slots of which value is determined by the width of the peak signal of the SC-PPM.

This demodulator architecture cannot efficiency BER performance under 87.5% and more of the dimming level since the peak value will be equal to the DC component that is filled the empty slots. This is one of the most challenges for the receiver scheme. It must be defined as two slot cases such as DC component and subcarrier filled to express the problem. For the DC component filled slot, an integral expression can be written as follows:

$$\boldsymbol{I_{DC}^{n} = bcTs} \quad ; \boldsymbol{n} = \{0,1,2,.....,\boldsymbol{M-1}\} \tag{9}$$

where, the c must be equal to b at a dimming level of 87.5% and more. Hence, both Eq. (9) and the integral of the SC-PPM signal indicated by Eq. (8) can be defined as,

$$\boldsymbol{I_{SC}^{n} = c^{2}Ts} \quad ; \boldsymbol{n} = \{0,1,2,.....,\boldsymbol{M-1}\} \tag{10}$$

where, it must be at a dimming level of 87.5% and more. As mentioned above, it is re-noted that the a value is equal to zero in the product process of the integral. Therefore, the demodulator scheme cannot efficiently operate at specified dimming levels. Eq. (4) can be also used to decide the condition of data bits for this demodulator model.

Improved Peak Detector based demodulator

This scheme has taken into account not only the peak value but also the bottom value of the a for the demodulation stage of the received SC-PPM signal to obstruct the challenges that emerged in the previous section. The difference between integrals taken in the period of a and c peak values determines the BER performance for this scheme. On the contrary to the previous section, this section assigns a non-zero value to the a parameter included by the subcarrier signal (SSC) used at the integration stage as shown in Eq. (8). To occur a difference between a and c parameters, the a value must be equal to the c in subcarrier signal that is used for demodulation process. The subcarrier signal acts as a DC component. Therefore, the integral result of Eq. (8) can be re-arranged by,

$$\begin{aligned} &\boldsymbol{T_{c}^{j} = nTs + j*Tsc} \quad ; \boldsymbol{n} = \{0,1,2,.....,\boldsymbol{M-1}\} \\ &\boldsymbol{and} \quad \boldsymbol{j} = \{0,1,2,.....,\boldsymbol{Ts/(M*Tsc)}\} \end{aligned} \tag{11}$$

$$\boldsymbol{T_{c}^{j+0,5} = nTs + \frac{(2j+1)*Tsc}{2}} \tag{12}$$

where, and are presented as starting and finish times. The j indicates the sequence of the filled slot of the subcarrier signal. A waveform is given to observe the starting time and finish time of the subcarrier signal in Fig. 3. By using Eqs.(11) and (12), the integral value of the slot can be given as follows:

$$\boldsymbol{I_{IPd}^{j} = \int_{T_{c}^{j}}^{T_{c}^{j+0,5}} S(t)S_{SC}(t)dt} \tag{13}$$

$$\boldsymbol{I_{IPd}^{j+0,5} = \int_{T_{c}^{j+0,5}}^{T_{c}^{j+1}} S(t)S_{SC}(t)dt} \tag{14}$$

$$\boldsymbol{I_{IPd}^{n} = \sum_{n=1}^{Ts/Tsc} \left(I_{IPd}^{j} - I_{IPd}^{j+0,5}\right)} \tag{15}$$

where, it is achieved a difference between filled and empty slots of the subcarrier signal. For the DC component, the result of Eq. (15) must be equal to zero. Yet, the slot by filled the subcarrier signal will get maximum value among the slots. Therefore, it can be used Eq. (6) to decide data bits from received the SC-PPM signal. Eq. (6) can be re-arranged as follows:

$$\boldsymbol{i = arg\,max\left\{I_{IPd}^{n}, I_{IPd}^{n+1}, ..., I_{IPd}^{M-1}\right\}} \quad ; \boldsymbol{n = 0} \tag{16}$$

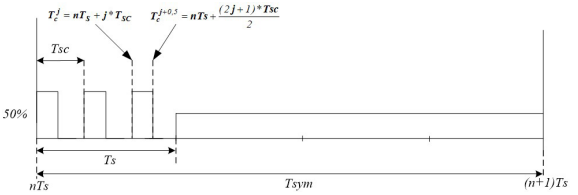

Figure 3. SC-4PPM signal waveform during one symbol period.

RESULTS AND DISCUSSION

This section gives the simulation results of the methods lengthy mentioned in the previous section. Three methods have been considered to apply to the SC-PPM receiver scheme to demodulate the received signal. We can briefly state the simulation results for these schemes according to their challenges.

In Fig. 4, it is given the simulation results that are obtained by taking into account the dimming level of the received SC-PPM signal. The dimming levels are including levels of 12.5%, 27.5%, 35%, 50%, 65%, 72.5%, and 87.5%. Fig. 4 (a) illustrates the simulation results under the dimming level of 12.5%. According to these results, the PD (Peak Detector) model has better BER performance than that of T-PPM (Traditional PPM) and IPD (Improved Peak Detector) schemes. It is shown from the results that the transmission distance can be increased from 2.52m to 2.75m at BER of about 10-5. A similar BER performance that is indicated in Fig. 4 (b) is obtained at the dimming level of 27.5%. Compared with Traditional PPM receiver, the PD can improve the transmission distance while the dimming level of the received signal is increased by up to 50%. At the dimming level of 27.5%, the transmission distance can be increased from 2.23m to 2.63m under the BER of 10-4. Another observation can be given related to the PD receiver model. When compared PD performances between dimming levels of 12.5% and 27.5%, it is shown that the PD model gives better BER performance at the dimming level of 12.5%.

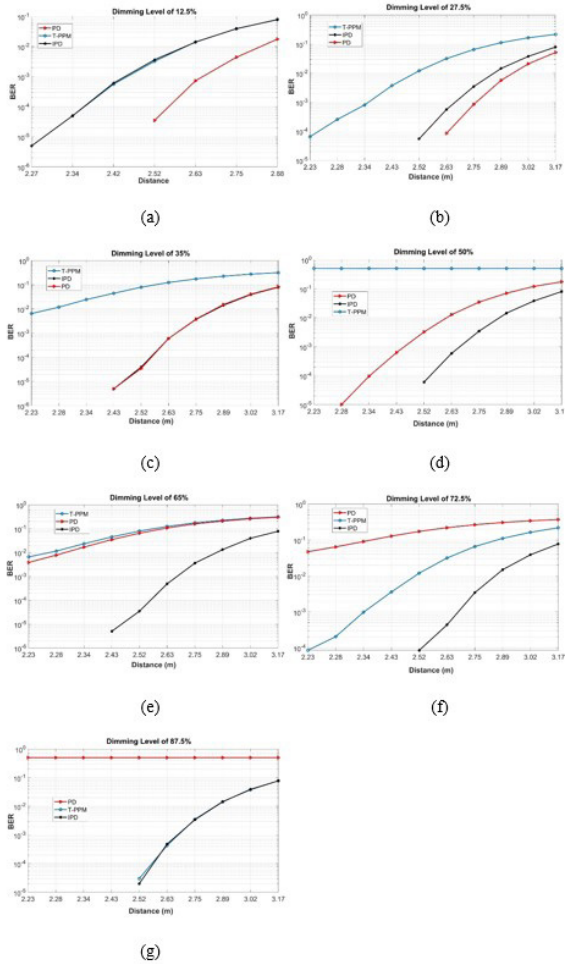

Figure 4. Simulation results versus the dimming level of the received signal.

The performance comparison given in Fig. 4 (c) shows that PD and IPD give similar BER performance. However, they have better performance compared with T-PPM. As shown in Fig. 4 (d), the T-PPM gives a meaningless BER performance since the integral values of the DC and the Subcarrier signal are equal to each other at the dimming level of 50%. This situation has been expressed in the previously mentioned section that clarifies the theoretical analysis of the receiver model. The simulation results for the dimming level of 65% are given in Fig. 4 (e) where the performance of IPD is the most efficient among the simulation results. According to performance analysis, PD and T-PPM give BER of approximately 10-3 at a distance of 2.23m while IPD has a similar BER performance at a distance of 2.75m. As shown in Fig. 4 (f), the BER performance of T-PPM is increasing for dimming levels that are above the dimming level of 50%. However, its BER performance can decrease at dimming levels above 87.5% since the gap between c and a has been converged. According to the last simulation result that is given in Fig. 4 (g), the peak detector (PD) has meaningless BER performance since the c value which is the peak value of the subcarrier signal is equal to b which is the peak value of the DC component. In addition to this, traditional PPM gives a similar BER performance to the IPD receiver. In brief, the IPD model cannot be affected by the dimming level of the received signal. It is a very useful characteristic under unknown dimming level cases. The BER performance of the T-PPM model is decreasing while the dimming level is changing from 12.5% to 50%. However, its performance can increase at dimming levels between 50% and 87.5% when the fullness of the received signal is raised.

In brief, the performance of the traditional PPM demodulator is increasing at the dimming levels between 50% and 87.5% since the difference between integral values of slot that is filled with subcarrier signal and the slot that is filled with DC signal is extending. The difference between DC value and c value is closing while the target brightness is rising. Hence, the performance of PD is gradually decreasing when the target dimming is approaching to dimming level of 87.5%. The difference between a and c steadies at the dimming levels between 12.5% and 87.5%. Therefore, the performance of IPD gives similar BER performance at brightness between these levels.

CONCLUSION

The paper has investigated the performance comparison of SC-PPM demodulator schemes that are PD, IPD, and T-PPM. The disadvantage of the T-PPM receiver is that it must be known the dimming level of the received SC-4PPM signal to successfully detect the bits. It is considered that this is a serious problem for real-time VLC systems. By using the PD scheme, the peak value of the subcarrier signal is detected. However, the performance of this receiver is decreasing while the dimming level of the received signal is increasing. The reason is that BER performance depends on the difference between the peak and bottom values of the subcarrier-filled slot. Hence, the IPD scheme is proposed to obtain a similar BER performance at all dimming levels between 12.5% and 87.5%. In the future, it can be improved a real-time system including these receiver models.

ACKNOWLEDGEMENT

The author received no financial support for the reseach, authorship, and/or puclication of this article.

CONFLICT OF INTEREST

Authors approve that to the best of their knowledge, there is not any conflict of interest or common interest with an institution/organization or a person that may affect the review process of the paper.

REFERENCES

1. Pratim Ray P. A perspective on 6G: Requirement, technology, enablers, challenges and future road map. Journal of Systems Architecture. 2021; 118: 102180. doi.org/10.1016/j.sysarc.2021.102180.
2. Sharma H, Jha RK. VLC Enabled Hybrid Wireless Network for B5G/6G Communications. Wireless Personal Communications. 2022;164: 1-31. doi. org/10.1007/s11277-021-09429-5.
3. Hakeem SAA, Hussein HH, Kim HW. Security Requirements and Challenges of 6G Technologies and Applications. Sensors. 2022; 22: 1-43. doi. org/10.3390/s22051969.
4. Xioang J, Lu L, Sun QT, Long K. Amplitude variation phenomenon in optical Physical-layer Network Coding with direct detection. Optics Communications. 2022; 505: 1-6. doi. org/10.1016/j.optcom.2021.127579.
5. Mishra S, Maheshwari R, Grover J, Vaishnavi J. Investigating the performance of a vehicular communication system based on visible light communication (VLC). International Journal of Information Technology. 2022; 14: 877-885. doi. org/10.1007/s41870-021-00834-4.
6. Oyewobi SS, Djouani K, Kurien AM. Visible Light Communications for Internet of Things: Prospects and Approaches, Challenges, Solutions and Future Directions. Technologies. 2022; 10: 1-18. doi.org/10.3390/technologies10010028.
7. Vijayalakshmi BA, Nesasudha M. Performance analysis of data transmission using LEDs over digital dimming modulation techniques in indoors. Optical and Quantum Electronics. 2022; 54: 1-12. doi.org/10.1007/s11082-022-03549-3.
8. Shaalan IE, Fadly EM, Aly MH. Enhanced ADO-OFDM-based adaptive digital dimming VLC system. Optica. 2022; 9: 2133-2136. doi.org/ 10.1364/OL.454339
9. Çelik Y. Quadrature Spatial Pulse Amplitude Modulation and Generalized Versions for VLC. EuropeanJournalofScienceand Technology.2021;21: 402-409. doi.org/10.31590/ejosat.793791.
10. Sadat H, Abaza M, Mansour A, Alfalou A. A Survey of NOMA for VLC Systems: Research Challenges and Future Trends. Sensors. 2022; 22: 1-23. doi. org/10.3390/s22041395
11. Alraih S, Shayea I, Behjati M, Nordin R, Abdullah NF, Samah AA, Nandi D. Revolution or Evolution?Technical Requirements and Considerations towards 6G Mobile Communications, Sensors. 2022; 22: 1-29. doi.org/ 10.3390/s22030762
12. Pan G, Ye J, Ding Z. Secure Hybrid VLC-RF Systems With Light Energy Harvesting. IEEE Transactions on Communications. 2017; 65: 4348 - 4359. doi. org/ 10.1109/TCOMM.2017.2709314
13. Xiao Y, Diamantoulakis PD, Fang Z, Hao L, Ma Z; Karagiannidis GK. Cooperative Hybrid VLC/RF Systems With SLIPT. IEEE Transactions on Communications. 2021; 69: 2532 - 2545. doi.org/10.1109/TCOMM.2021.3051908.
14. Bao X, Dai J, Zhu X. Visiblelightcommunicationsheterogeneous network (VLC-HetNet): new model and protocols for mobile scenario. Wireless Networks. 2017; 23: 299-309. doi.org/10.1007/s11276-016-1233-z.
15. Kashef M, Ismail M, Abdallah M, Qaraqe KA, Serpedin E. Energy Efficient Resource Allocation for Mixed RF/VLC Heterogeneous Wireless Networks. IEEE Journal on Selected Areas in Communications. 2016; 34: 883-893. doi. org/10.1109/JSAC.2016.2544618.
16. Yeşilkaya A, Miramirkhani F, Alsan HF, Başar E, Panayırcı E, Uysal M. Görünür Işık Kanallarının Modellenmesi ve Optik OFDM Sistemleri için Başarım Analizi. EMO Bilimsel Dergi. 2015; 5: 1-11.
17. NamdarM,BasgumusA,TsiftsisT,AltuncuA.Outageand BER performances of indoorrelay-assisted hybrid RF/VLC systems. IET Communications. 2018; 12: 2104-2109. doi.org/10.1049/iet-com.2018.5389
18. Sönmez, M. Performance Analysis of FSK-PPM Technique in Visible-Light Communication Systems. Journal of Optical Communications. 2022; 43: 447-455. doi.org/10.1515/joc-2019-0009.
19. Oyewobi SS, Djouani K, Kurien AM. Visible Light Communications for Internet of Things: Prospects and Approaches, Challenges, Solutions and Future Directions. Technologies. 2022; 10: 1-18. doi.org/10.3390/technologies10010028.
20. Gözüaçık E, Görkem L. Görünür Işık Haberleşmesi ile şç Mekan Konum Belirleme. Journal of New Results in Engineering and Natural Science. 2020; 11: 23-35.
21. Kimyacı M, Çürük SM. Çoklu Vericili Görünür Işık Haberleşmesinde Kanal. Academic Platform Journal of Engineering and Science. 2020; 9: 10-18. doi.org/10.21541/apjes.779495.
22. Bilim M. Approximate ASER analysis of MIMO TAS/MRC networks over Weibull fading channels. Annals of Telecommunications. 2021; 76: 73-81. doi.org/10.1007/s12243-020-00810-2.
23. Miramirkhani F, Uysal M. Channel Modeling and Characterization for Visible Light Communications. IEEE Photonics Journal. 2015; 7: 1-16. doi.org/ 10.1109/JPHOT.2015.2504238.
24. Das D, Mandal SK. Dimming controlled multi header hybrid PPM (MH-HPPM) for visible light communication. Optical and Quantum Electronics. 2021; 123: 1-18. doi.org/10.1007/s11082-021-02758-6.
25. Lee K., Park H. Modulations for Visible Light Communications With Dimming Control. IEEE Photonics Technology Letters. 2011; 23: 1136-1138. doi.org/10.1109/LPT.2011.2157676.
26. Sugiyama H, Haruyama S, Nakagawa M. Brightness Control Methods for Illumination and Visible-Light Communication Systems. Proceedings of the Third International Conference on Wireless and Mobile Communications Physical Communication, Guadeloupe, 4-9 March, pp: 1-6, 2007.
27. Sugiyama H, Haruyama S, Nakagawa, M. Experimental investigation of modulation method for visible-light communications. IEICE Trans. Commun. 2006; 12: 3393– 3400. doi.org/10.1093/ietcom/e89-b.12.3393.
28. Belli R, Runge C, Portugheis J, Finamore W. A capacity-approaching coding scheme

for M-PAM VLC systems with dimming control. Optics Communications. 2022; 509: 1-5. doi. org/10.1016/ j.optcom.2021.127891.

29. Kim S, J SY. Novel FEC Coding Scheme for Dimmable Visible Light Communication Based on the Modified Reed–Muller Codes. IEEE Photonics Technology Letters. 2011; 23: 1514-1516. doi. org:/10.1109/LPT.2011.2163625
30. Lin C, Zhu Y, Zhang Y. An Appropriate Modulation Scheme for High Density Visible Light Communication System. 4th International ConferenceonMachinery,Materialsand ComputingTechnology, Hangzhou, 23-24 January, pp. 1108-1112, 2016.
31. Irfanud D, Kim H. Energy-efficient brightness control and data transmission for visible light communication. IEEE photonics technology letters. 2014; 26: 781-784. doi.org/10.1109/ LPT.2014.2306195.
32. Li F, Wu K, Zou W, Chen J. Optimization of LED's SAHPs to simultaneously enhance SNR uniformity and support dimming control for visible light communication. OpticsCommunications. 2015;341:218-227. doi.org/10.1016/j.optcom.2014.12.025.
33. Li F, Wu K, Zou W, Chen J.. Analysis of energy saving ability in dimming VLC systems using LEDs withoptimizedSAHP.Optics Communications.2016;361: 86-96. doi.org/10.1016/j.optcom.2015.10.045.
34. Sönmez, M. Görünür Işık Haberleşme Sistemleri için SC-PPM Teknişi Kullanılarak Alıcı-Verici Tasarımı. BEÜ Fen Bilimleri Dergisi, 2021; 10: 126-132. doi.org/10.17798/bitlisfen.682538.
35. Aşır TT, Sönmez M. The modulation classification methods in PPM–VLC systems. Optical and Quantum Electronics. 2023; 53: 1-20. doi.org/ 10.21203/rs.3.rs-1877887/v1